



Ballistic transport of interacting Bose particles in a tight-binding chain

P. S. Muraev ^{1,2}, D. N. Maksimov,^{1,3} and A. R. Kolovsky ^{1,2}

¹*Kirensky Institute of Physics, Federal Research Center KSC SB RAS, 660036 Krasnoyarsk, Russia*

²*School of Engineering Physics and Radio Electronics, Siberian Federal University, 660041 Krasnoyarsk, Russia*

³*IRC SQC, Siberian Federal University, 660041 Krasnoyarsk, Russia*



(Received 16 July 2022; accepted 17 November 2022; published 6 December 2022)

It is known that the quantum transport of noninteracting Bose particles across a tight-binding chain is ballistic in the sense that the current does not depend on the chain length. We address the question whether the transport of *strongly interacting* bosons can be ballistic as well. We find such a regime and show that, classically, it corresponds to the synchronized motion of local nonlinear oscillators. It is also argued that, unlike the case of noninteracting bosons, the transporting state responsible for the ballistic transport of interacting bosons is metastable, i.e., the current decays in the course of time. An estimate for the decay time is obtained.

DOI: [10.1103/PhysRevE.106.064203](https://doi.org/10.1103/PhysRevE.106.064203)

I. INTRODUCTION

In the past decade much effort has been invested in understanding the quantum transport of Bose particles across a one-dimensional lattice connecting two particle reservoirs [1–7]. Several theoretical approaches have been used to analyze this problem, including straightforward numerical simulations of the master equation for bosons in the lattice, quantum jump methods, and the semiclassical (mean-field) and pseudoclassical approaches. The last two approaches are especially important for developing an intuitive physical picture because they map the quantum transport problem to the classical problem of excitation transfer in a chain of coupled nonlinear oscillators with the edge oscillators driven by external forces, where the type of driving force is determined by the ergodic properties of the particle reservoirs. Namely, if reservoirs justify the Born-Markov approximation, the edge oscillators are driven by the complex white noise whose intensity is proportional to the particle density in the reservoir [1–3]. For non-Markovian reservoirs the white noise has to be superseded by the narrow-band noise with the spectral density spanning a finite frequency interval [4]. Typically, this is the case where Bose particles in reservoirs are close to condensation. At last, one may consider the situation where the spectral density of the colored noise is given by the δ function, i.e., we have a periodic driving. Experimentally, this case is realized, for example, in a chain of capacitively coupled transmons where the first transmon is excited by a microwave generator [8–10], or in an array of optical cavities with the Kerr nonlinearity where the first cavity is excited by a laser. We mentioned that the minimal-size chains consisting of two cavities are currently used to study a number of other fundamental problems [11–17]. In the present paper, however, we focus exclusively on the transport problem where the main question is the current of Bose particles across the chain. As the main result, we show that edge-driven systems can exhibit an exotic transport regime where the current of *strongly*

interacting bosons is independent of the chain length and is insensitive to a weak disorder. This relates the reported results to the problem of superfluidity of Bose gases [18,19].

II. THE MODEL

We consider a chain of coupled nonlinear quantum oscillators of a finite length L , where the first oscillator in the chain is driven by a monochromatic field while the last oscillator is subject to decay. Referring to laboratory systems, this model describes, for example, the chain of coupled transmons where the first transmon is excited by the microwave field and the transmitted signal is read from the last transmon. In the rotating-wave approximation the quantum Hamiltonian of the system under scrutiny has the form

$$\begin{aligned} \widehat{\mathcal{H}} = & \sum_{\ell=1}^L \hbar(\omega_{\ell} - \nu)\hat{n}_{\ell} - \frac{\hbar J}{2} \left(\sum_{\ell=1}^{L-1} \hat{a}_{\ell+1}^{\dagger} \hat{a}_{\ell} + \text{H.c.} \right) \\ & + \frac{\hbar^2 U}{2} \sum_{\ell=1}^L \hat{n}_{\ell}(\hat{n}_{\ell} - 1) + \frac{\sqrt{\hbar}\Omega}{2} (\hat{a}_1^{\dagger} + \hat{a}_1), \quad (1) \end{aligned}$$

where the index ℓ labels the chain site, \hat{a}_{ℓ} and \hat{a}_{ℓ}^{\dagger} are the creation and annihilation bosonic operators commuting to unity, $\hat{n}_{\ell} = \hat{a}_{\ell}^{\dagger} \hat{a}_{\ell}$ is the number operators, ω_{ℓ} are the linear frequencies (on-site energies), J is the hopping matrix element, U the interaction constant (nonlinearity), and the Rabi frequency Ω characterizes the strength of the external monochromatic driving with the frequency ν . We shall denote the detuning $\nu - \omega_{\ell}$ by Δ_{ℓ} where the absence of the subindex ℓ will imply identical on-site energies.

Since only the last oscillator is subject to decay, the governing master equation for the system density matrix $\widehat{\mathcal{R}}$ reads

$$\frac{\partial \widehat{\mathcal{R}}}{\partial t} = -\frac{i}{\hbar} [\widehat{\mathcal{H}}, \widehat{\mathcal{R}}] - \frac{\gamma}{2} (\hat{a}_L^{\dagger} \hat{a}_L \widehat{\mathcal{R}} - 2\hat{a}_L \widehat{\mathcal{R}} \hat{a}_L^{\dagger} + \widehat{\mathcal{R}} \hat{a}_L^{\dagger} \hat{a}_L), \quad (2)$$

where γ is the relaxation constant. We mention in passing that the results reported below also hold true in the case where the other oscillators are also subject to decay but their decay rates $\gamma_\ell \ll \gamma$. To address the quantum-to-classical correspondence, we incorporate in the Hamiltonian (1) and the master equation (2) the effective Planck constant \hbar , the physical meaning of which will be explained in the beginning of Sec. V.

Our main object of interest is the single-particle density matrix (SPDM)

$$\hat{\rho}(t) = \text{Tr}[\hat{a}_\ell^\dagger \hat{a}_m \mathcal{R}(t)]. \quad (3)$$

The diagonal elements of this matrix give the occupation numbers of the chain sites while the subdiagonal determines the current across the chain,

$$j(t) = \frac{1}{L-1} \text{Tr}[\hat{j} \hat{\rho}(t)], \quad (4)$$

where \hat{j} is the single-particle current operator with the elements $j_{\ell,\ell'} = J(\delta_{\ell,\ell'+1} - \text{H.c.})/2i$. At the same time, as it follows from the continuity equation, the stationary current $\bar{j} = j(t \rightarrow \infty)$ is given by the stationary population of the last site multiplied by γ , i.e., $\bar{j} = \gamma |a_L|^2$.

III. SEMICLASSICAL ANALYSIS

The semiclassical approximation associates the mean values of the creation and annihilation operators times $\sqrt{\hbar}$ with the conjugated canonical variables a_ℓ and a_ℓ^* . Then the governing (Gross-Pitaevskii) equations take the form

$$\begin{aligned} i\dot{a}_1 &= (-\Delta + U|a_1|^2)a_1 - \frac{J}{2}a_2 + \frac{\Omega}{2}, \\ i\dot{a}_\ell &= (-\Delta + U|a_\ell|^2)a_\ell - \frac{J}{2}(a_{\ell+1} + a_{\ell-1}), \\ i\dot{a}_L &= (-\Delta + U|a_L|^2)a_L - \frac{J}{2}a_{L-1} - i\frac{\gamma}{2}a_L. \end{aligned} \quad (5)$$

Due to contraction of the phase volume for $\gamma \neq 0$, an arbitrary trajectory $\mathbf{a}(t)$ evolves to some attractor in the multidimensional phase space of the system [20,21]. In what follows we focus on attractors which ensure the ballistic transport of excitations from the first to the last oscillator. We begin with the case of the vanishing interparticle interaction where the system has a single attractor—a simple focus.

A. Vanishing interparticle interaction

For $U = 0$ the system of coupled differential equations (5) can be decoupled by introducing the new canonical variables given by the eigenmodes $X_\ell^{(j)}$ of the undriven ($\Omega = 0$) chain. Since we excite the first oscillator and the stationary current is proportional to the squared amplitude of the last oscillator, we have

$$\bar{j} \sim \left| \sum_{n=1}^L \frac{X_1^{(n)} X_L^{(n)}}{\Delta - \epsilon_n} \right|^2, \quad (6)$$

where ϵ_n are the chain complex eigenfrequencies with $\text{Re}[\epsilon_n] \approx -J \cos(\pi n/L)$ and $\text{Im}[\epsilon_n] \sim \gamma$. It follows from Eq. (6) that the stationary current as a function of the detuning shows L peaks in the interval $|\Delta| < J/2$ —the phenomenon

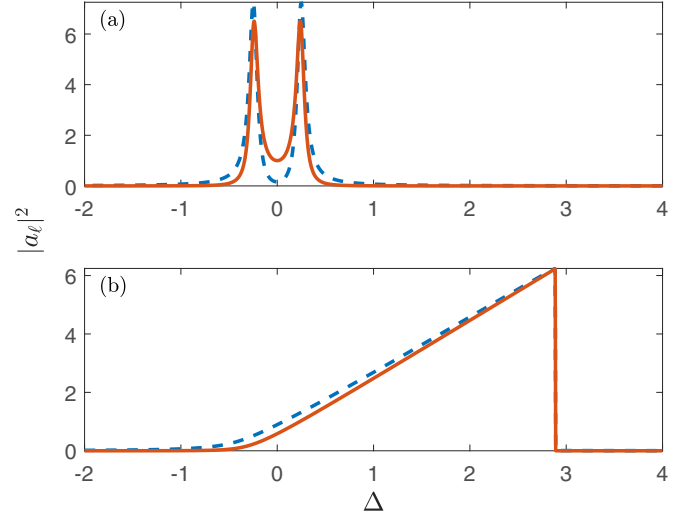


FIG. 1. Stationary values of the squared amplitudes in a chain of length $L = 2$ as a function of the detuning Δ are shown by the dashed and solid lines for $U = 0$ in (a), and $U = 0.5$ in (b). The parameters are $J = 0.5$, $\gamma = 0.2$, and $\Omega = 0.5$. The current across the chain is proportional to $|a_2|^2$ depicted by the red solid line.

known as resonant transmission. Resonant transmission is illustrated in Fig. 1(a) for $L = 2$. If $|U| \ll J$, the transmission peaks slightly bend to the left or right, depending on the sign of U . However, with a further increase of the interaction constant, the discussed simple attractor shows a cascade of bifurcations [22], leading to a number of qualitatively different transport regimes. We also would like to mention that the resonant transmission Eq. (6) is sensitive to the on-site disorder ω_ℓ due to the presence of the product $X_1^{(n)} X_L^{(n)}$ in Eq. (6), which tends to zero in the regime of Anderson's localization.

B. Strong interparticle interaction

Next, we address the case $|U| > J$ and, to be specific, we shall consider positive U from now on. In this case the attractor, which ensures the ballistic transport, corresponds to the synchronized motion of the oscillators,

$$a_{\ell+1} \approx a_\ell e^{i\phi}, \quad \phi \approx \arcsin(\gamma/J). \quad (7)$$

Equation (7) is illustrated in Fig. 2 for $L = 8$ and in Fig. 1(b) for $L = 2$. The crucial feature of the solution (7), which later on will be referred to as the transporting state, is the existence of the critical detuning Δ_{cr} above which the basin of the discussed attractor shrinks to zero.

Let us discuss the results shown in Fig. 1(b) in more detail. First, we notice that in the interval $0 < \Delta < \Delta_{\text{cr}}$ the squared amplitudes $|a_\ell|^2$ grow approximately linear with the detuning, i.e., $|a_\ell|^2 \approx \Delta/U$. For $\gamma = 0$ this linear dependence exhibits the phenomenon of capturing in the nonlinear resonance [20,21]. In the presence of dissipation, however, the nonlinear resonance degenerates into the limit cycle. This transformation of the nonlinear resonance into the limit cycle can be studied in full detail for $L = 1$, i.e., for the dissipative driven nonlinear oscillator. In that system the stationary

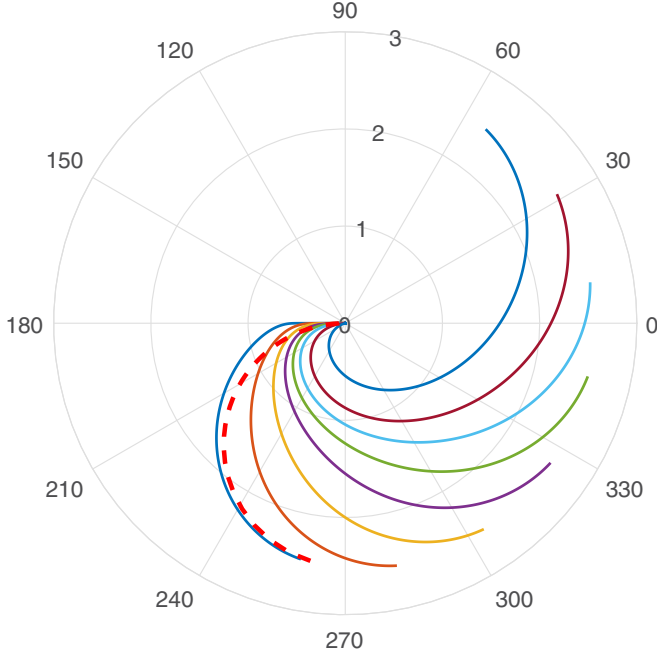


FIG. 2. The stationary complex amplitude of the local oscillators in a chain of length $L = 8$ for $-4 < \Delta < 2.5$. The dashed line is Eq. (8). The other system parameters are as in Fig. 1.

amplitude of the oscillator is given by the relation [23]

$$a = \frac{\Omega/2}{U|a|^2 - \Delta - i\gamma/2}, \quad (8)$$

where $|a|^2$ obeys the algebraic equation

$$|a|^2 = \frac{(\Omega/2)^2}{(U|a|^2 - \Delta)^2 + (\gamma/2)^2}. \quad (9)$$

We found that Eqs. (8) and (9) provide a good approximation for the amplitude of the first oscillator in the chain if $L > 1$ (see the dashed line in Fig. 2). Thus, we can use Eq. (9) to obtain an estimate for Δ_{cr} ,

$$\Delta_{\text{cr}} \approx U(\Omega/\gamma)^2. \quad (10)$$

It is seen in Fig. 1(b) that, when we exceed this critical value, the amplitude of the last oscillator in the chain drops almost to zero, which results in the abrupt decrease of the current.

C. Basin size

For future purposes we need to know the basin of the discussed attractor. Although visualizing the attractor basin in a multidimensional phase space is difficult, one can easily estimate its size [24]. To do this we randomly perturbed the stationary amplitude of the last oscillator as $a_L \rightarrow a_L + \xi$, where ξ samples the Gaussian distribution with the width σ , and checked whether the perturbed trajectory attracts back to the solution (7). Approximating the attractor basin by the circle (more precisely, the basin projection on the a_L plane) we expect that the number of not-attracted trajectories grows with an increase of σ as

$$S \sim \sigma^2 \exp\left(-\frac{r^2}{2\sigma^2}\right), \quad (11)$$

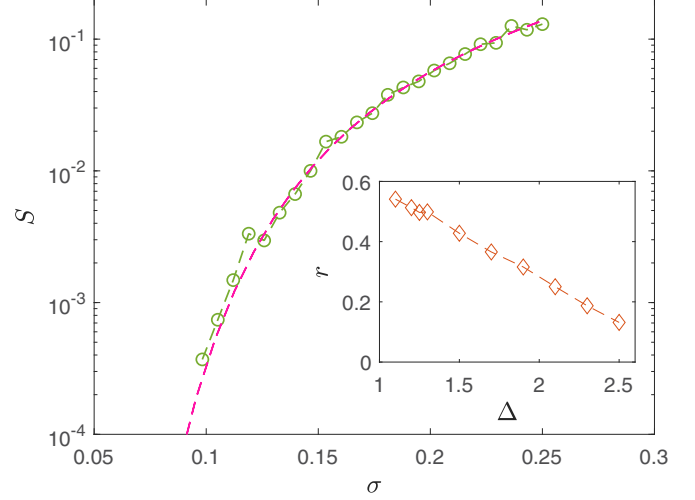


FIG. 3. Main panel: Approximation of the numerical data by the function (11) for $\Delta = 1.90$. Inset: The basin size as a function of the detuning Δ . The system parameters are the same as in Fig. 1.

where r is the circle radius. Next, interpolating the numerical data by the function (11) we find $r = r(\Delta)$ (see Fig. 3). It is seen in Fig. 3 that the basin size decreases approximately linearly with Δ .

D. Adiabatic passage

We conclude this section by a remark that the results presented in Figs. 1 and 2 can be fairly reproduced by using the adiabatic passage where the detuning Δ is slowly changed in time. For the figure parameters we found no difference between the stationary and quasistationary solutions if the sweeping β ,

$$\beta = d\Delta/dt,$$

is smaller than 100 tunneling periods $T = 2\pi/J$ per unit interval of Δ . It should be also stressed that, since we chose $U > 0$, we consider positive β . Specifically, in our adiabatic protocol we started from $\Delta = -4$ and $a_\ell = 0$. Then, Δ was increased with the rate $\beta = 1.2 \times 10^{-3}$ leading to results identical to those in Figs. 1 and 2. If the sweeping direction were inverted, we would observe very different dynamical regimes, including the limit cycle in the frequency interval $0.37 < \Delta < 0.78$ ($L = 2$) where the oscillator amplitudes periodically change in time [25].

IV. QUANTUM DYNAMICS

In this section we compare the results of the semiclassical analysis with the solution of the master equation (2). We solve the master equation in the Hilbert space given by the direct sum of the subspaces associated with the fixed number of particles in the chain, $N = 0, 1, \dots, N_{\text{max}}$, where N_{max} is the truncation parameter. We control the accuracy by checking the convergence of the results as N_{max} is increased.

First, we study the transporting state of the system for $U = 0$. We find this state by sweeping the detuning Δ with a fixed rate β in the interval $|\Delta| \gg J$. We take the precaution that the rate β is small enough to ensure the adiabatic regime. The

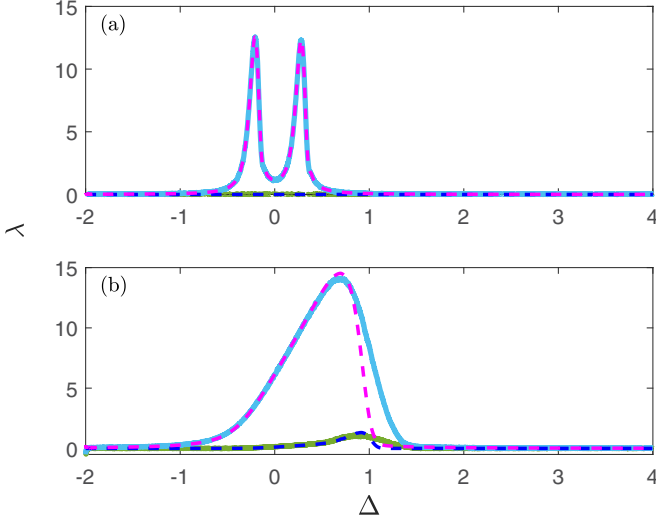


FIG. 4. Eigenvalues of the SPDM for $U = 0$ and $\hbar = 1$ (top) and $U = 0.5$ and $\hbar = 0.25$ (bottom). The sweeping rate of the detuning Δ is $\beta = 1.2 \times 10^{-3}$. The dashed and solid lines are the exact result and the result of the pseudoclassical approach (average over 3600 realizations), respectively.

upper panel in Fig. 4 shows eigenvalues $\lambda_n = \lambda_n(\Delta)$ of the stationary SPDM of the system with $L = 2$ sites. Notice that the matrix has only one nonzero eigenvalue and this holds true for arbitrary L . Comparing the result shown in Fig. 4(a) with the result of the semiclassical analysis we conclude that the stationary SPDM is determined by the stationary solution $\tilde{\mathbf{a}} = \mathbf{a}(t \rightarrow \infty)$ of the classical Eqs. (5) through the relation $\hat{\rho}_{\ell,m} \sim \tilde{a}_\ell^* \tilde{a}_m$.

Next, we consider the case $U = 0.5$ where we expect similarities with the result depicted in the bottom panel in Fig. 1. Indeed, it is seen in Fig. 4(b) that the number of bosons in the chain (which is given by $\text{Tr}[\hat{\rho}] = \sum_n \lambda_n$) initially grows linearly with Δ , however, for $\Delta \approx 1.0$ it drops back to zero. We also notice that for $U \neq 0$ the system SPDM may differ from a pure state, i.e., $\lambda_2 \neq 0$.

Summarizing the obtained results, we come to the following intermediate conclusion. One finds an excellent agreement between the classical and quantum approaches in the case $U = 0$ and a strong discrepancy in the case $U \neq 0$. In the next section we quantify this discrepancy by using the pseudoclassical approach.

V. PSEUDOCCLASSICAL APPROACH

First, we clarify the meaning of the effective Planck constant entering Eqs. (1) and (2). It follows from these equations that the actual parameters, which determine the quantum dynamics, are $U' = \hbar U$ and $\Omega' = \Omega/\sqrt{\hbar}$. Remarkably, the indicated scaling of the interaction constant and the Rabi frequency does not alter the classical dynamics of the system where we associate operators $\sqrt{\hbar}\hat{a}$ and $\sqrt{\hbar}\hat{a}^\dagger$ with the canonical variables a and a^* . Thus, the effective Planck constant \hbar determines the mean number of bosons in the system. The larger is this number, the closer is the quantum system to its classical counterpart. The pseudoclassical approach is

an approximation to the exact quantum dynamics through a series expansion in the parameter \hbar . It substitutes the master equation for the system density matrix by the Fokker-Planck equation for the classical distribution function $f = f(\mathbf{a}, \mathbf{a}^*, t)$ and, in this sense, is equivalent to the truncated Wigner function approximation [26–29] in the single-particle quantum mechanics. Explicitly, we have [4]

$$\frac{\partial f}{\partial t} = \{\mathcal{H}, f\} + \frac{\gamma}{2} \left[\frac{\partial(a_L f)}{\partial a_L} + \frac{\partial(a_L^* f)}{\partial a_L^*} \right] + \frac{\hbar\gamma}{2} \frac{\partial^2 f}{\partial a_L \partial a_L^*}, \quad (12)$$

where

$$\mathcal{H} = \sum_{\ell=1}^L \left[-(\Delta + \hbar U) |a_\ell|^2 + \frac{U}{2} |a_\ell|^4 \right] - \frac{J}{2} \sum_{\ell}^L (a_{\ell+1}^* a_\ell + \text{c.c.}) + \frac{\Omega}{2} (a_1 + a_1^*), \quad (13)$$

and $\{\dots, \dots\}$ denote the Poisson brackets.

Let us discuss the meaning of different terms in the displayed equation. The first term on the right-hand side of this equation is the Liouville equation for the conservative chain. The second term describes the contraction of the phase volume in the dissipative chain and thus can be referred to as friction. Finally, the last term describes the diffusion. Using Eq. (12) the SPDM is found as the phase-space average,

$$\rho_{\ell,m}(t) = \int a_\ell^* a_m f(\mathbf{a}, \mathbf{a}^*, t) d\mathbf{a} d\mathbf{a}^*. \quad (14)$$

Usually, one evaluates the multidimensional integral in Eq. (14) by putting into correspondence to the Fokker-Planck equation (12) the following Langevin equation,

$$i\dot{a}_\ell = \frac{\partial H}{\partial a_\ell^*} - i\frac{\gamma}{2} \delta_{\ell,L} a_\ell + \sqrt{\frac{\hbar\gamma}{2}} \delta_{\ell,L} \xi(t), \quad (15)$$

where $\xi(t)$ is the δ -correlated white noise. Then the elements of SPDM are calculated as

$$\rho_{\ell,m}(t) = \overline{a_\ell^*(t) a_m(t)} - \frac{1}{2} \delta_{\ell,m}, \quad (16)$$

where the bar denotes the average over different realizations of the stochastic force $\xi(t)$.

A. Comparison with the exact results

The primary advantage of the pseudoclassical approach as compared to the straightforward solution of the master equation is the simplicity of numerical simulations which allows us to go deep in the semiclassical region. Of course, on the quantitative level, the pseudoclassical approach gives some systematic error. However, on the qualitative level, it correctly reproduces all main results of the quantum analysis. We illustrate this statement in the lower panel in Fig. 4 where we compare the SPDM calculated by using the pseudoclassical approach (solid lines) with the exact result (dashed lines) for $\hbar = 0.25$. It is seen in Fig. 4(b) that the pseudoclassical approach correctly captures the decay of the SPDM long before Δ_{cr} . In the next section we use it to study this decay

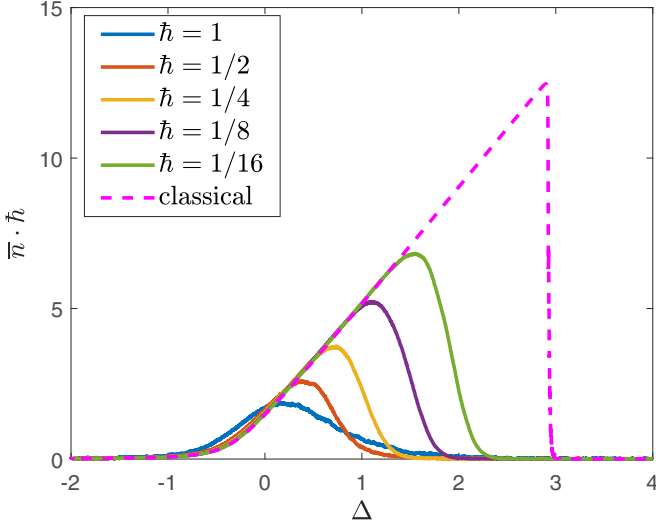


FIG. 5. The mean number of bosons in the dimer times the effective Planck constant according to the pseudoclassical approach (solid lines, average over 3600 realizations) for different values of the effective Planck constant. The other system parameters are $J = 0.5$, $U = 0.5$, $\Omega = 0.5$, $\gamma = 0.2$, and the sweeping rate $\beta = 1.2 \times 10^{-3}$. The dashed line shows the classical result.

for the values of the effective Planck constant which are inaccessible in the exact quantum simulations. In fact, within the pseudoclassical approach the variation of the effective Planck constant affects only the noise intensity while in the quantum equation of motion it rescales the interparticle interaction and the amplitude of the driving force, which requires a proportional increase of the truncation parameter N_{\max} .

B. Lifetime of the transporting state

The quantum dynamics of the system calculated by using the pseudoclassical approach is exemplified in Fig. 5. Shown are the mean number of bosons in the chain \bar{n} , $\bar{n} = \text{Tr}[\hat{\rho}] = \sum_n \lambda_n$, times the effective Planck constant. It is seen that for $\hbar \rightarrow 0$ the quantum dynamics converges to the classical result, where the destruction of the ballistic transport takes place at $\Delta_{\text{cr}} \approx 3.0$. The results depicted in Fig. 5 suggest the other critical detuning,

$$\Delta_{\text{qu}} = \Delta_{\text{qu}}(\hbar, \beta) \leq \Delta_{\text{cr}},$$

at which the numbers of bosons in the chain are maximal. The fundamental reason for the inequality $\Delta_{\text{qu}} \leq \Delta_{\text{cr}}$ is the metastable character of the quantum attractor associated with the discussed transporting state.

To determine the lifetime $\tau = \tau(\Delta, \hbar)$ of the transporting state we evolve the system to $\Delta < \Delta_{\text{qu}}$ and then fix this detuning for the rest of time (see Fig. 6). Then, by approximating the decay dynamics by the exponential function, we extract τ . The dependence of the lifetime τ on Δ is depicted in the inset in Fig. 6. This result suggests the following estimate for the lifetime,

$$\tau \sim \exp\left(\frac{r}{\hbar}\right), \quad (17)$$

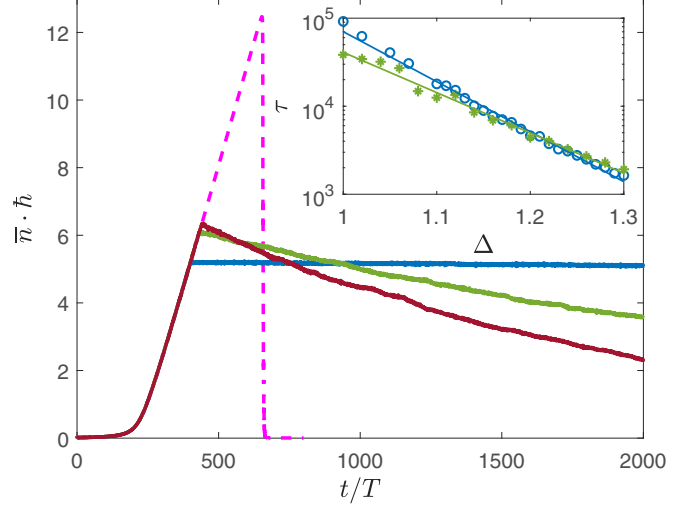


FIG. 6. Main panel: The mean number of bosons in the dimer times the effective Planck constant as a function of time for $\Delta = 1$ (blue line), $\Delta = 1.24$ (green line), and $\Delta = 1.30$ (brown line). The value of the effective Planck constant $\hbar = 1/16$. The dashed line shows the result in the classical limit. The inset shows the lifetime of the transporting state as the function of Δ for $L = 2$ (open circles) and $L = 8$ (asterisks).

where $r = r(\Delta)$ is the basin size of the classical attractor. Roughly, Eq. (17) compares the minimal-size wave packet with the basin size, and to ensure the exponentially long lifetime of the considered transporting state, one should satisfy the condition $r(\Delta) \gg \hbar$.

C. Long chain

We repeated the above numerical simulations for the chain of length $L = 8$ and obtained essentially the same results (see the inset in Fig. 6). The only different aspect is that for a long chain we can address the Anderson problem. It was found that the discussed transporting state is insensitive to a weak on-site disorder $|\omega_\ell - \omega| \leq \epsilon \ll \Delta$. One finds a qualitative explanation for this result in terms of the synchronization theory. In fact, the considered system of coupled nonlinear oscillators can be viewed as one of the physical realizations of the Kuramoto model [30]. The important property of the Kuramoto model is that synchronization may occur for oscillators with different eigenfrequencies. In our case this means that the nonlinear oscillators will be synchronized also in the presence of an on-site disorder, i.e., different linear frequencies ω_ℓ .

VI. CONCLUSION

We study the transport of interacting Bose particles in the open Bose-Hubbard chain where the particles are injected in the first site of the chain and withdrawn from the last site. The analysis is done by using the pseudoclassical approximation which puts in correspondence to the open Bose-Hubbard model the chain of coupled nonlinear oscillators and where the transport of particles corresponds to the transport of excitations from the first to the last oscillator. It is shown that one can observe the ballistic transport of excitations by capturing the system into the classical attractor which describes the synchronized oscillators. The quantum counterpart of this

attractor corresponds to the quantum transporting state which, however, has a finite lifetime as seen in Fig. 6. We obtain an estimate [Eq. (17)] for the lifetime of this state and argue that it becomes exponentially long in the pseudoclassical limit.

ACKNOWLEDGMENT

This work has been supported by Russian Science Foundation through Grant No. N19-12-00167.

-
- [1] A. Ivanov, G. Kordas, A. Komnik, and S. Wimberger, Bosonic transport through a chain of quantum dots, *Eur. Phys. J. B* **86**, 345 (2013).
- [2] G. Kordas, D. Witthaut, P. Buonsante, A. Vezzani, R. Burioni, A. Karanikas, and S. Wimberger, The dissipative Bose-Hubbard model, *Eur. Phys. J.: Spec. Top.* **224**, 2127 (2015).
- [3] A. R. Kolovsky, Z. Denis, and S. Wimberger, Landauer-Büttiker equation for bosonic carriers, *Phys. Rev. A* **98**, 043623 (2018).
- [4] A. A. Bychek, P. S. Muraev, D. N. Maksimov, and A. R. Kolovsky, Open Bose-Hubbard chain: Pseudoclassical approach, *Phys. Rev. E* **101**, 012208 (2020).
- [5] P. S. Muraev, D. N. Maksimov, and A. R. Kolovsky, Resonant transport of bosonic carriers through a quantum device, *Phys. Rev. A* **105**, 013307 (2022).
- [6] L. Amico, M. Boshier, G. Birkel, A. Minguzzi, C. Miniatura, L.-C. Kwek, D. Aghamalyan, V. Ahufinger, D. Anderson, N. Andrei, A. S. Arnold, M. Baker, T. A. Bell, T. Bland, J. P. Brantut, D. Cassettari, W. J. Chetcuti, F. Chevy, R. Citro, S. D. Palo *et al.*, Roadmap on Atomtronics: State of the art and perspective, *AVS Quantum Sci.* **3**, 039201 (2021).
- [7] J. W. Z. Lau, K. S. Gan, R. Dumke, L. Amico, L.-C. Kwek, and T. Haug, Atomtronic multi-terminal Aharonov-Bohm interferometer, [arXiv:2205.01636](https://arxiv.org/abs/2205.01636).
- [8] J. Raftery, D. Sadri, S. Schmidt, H. Türeci, and A. A. Houck, Observation of a Dissipation-Induced Classical to Quantum Transition, *Phys. Rev. X* **4**, 031043 (2014).
- [9] M. Fitzpatrick, N. M. Sundaresan, A. C. Y. Li, J. Koch, and A. A. Houck, Observation of a Dissipative Phase Transition in a One-Dimensional Circuit QED Lattice, *Phys. Rev. X* **7**, 011016 (2017).
- [10] G. P. Fedorov, S. V. Remizov, D. S. Shapiro, W. V. Pogosov, E. Egorova, I. Tsitsilin, M. Andronik, A. A. Dobronosova, I. A. Rodionov, O. V. Astafiev, and A. V. Ustinov, Photon Transport in a Bose-Hubbard Chain of Superconducting Artificial Atoms, *Phys. Rev. Lett.* **126**, 180503 (2021).
- [11] K. G. Lagoudakis, B. Pietka, M. Wouters, R. André, and B. Deveaud-Plédran, Coherent Oscillations in an Exciton-Polariton Josephson Junction, *Phys. Rev. Lett.* **105**, 120403 (2010).
- [12] M. Abbarchi, A. Amo, V. Sala, D. Solnyshkov, H. Flayac, L. Ferrier, I. Sagnes, E. Galopin, A. Lemaître, G. Malpuech, and J. Bloch, Macroscopic quantum self-trapping and Josephson oscillations of exciton polaritons, *Nat. Phys.* **9**, 275 (2013).
- [13] B. Cao, K. W. Mahmud, and M. Hafezi, Two coupled nonlinear cavities in a driven-dissipative environment, *Phys. Rev. A* **94**, 063805 (2016).
- [14] W. Casteels and C. Ciuti, Quantum entanglement in the spatial-symmetry-breaking phase transition of a driven-dissipative Bose-Hubbard dimer, *Phys. Rev. A* **95**, 013812 (2017).
- [15] S. R. K. Rodriguez, W. Casteels, F. Storme, N. Carlon Zambon, I. Sagnes, L. Le Gratiet, E. Galopin, A. Lemaître, A. Amo, C. Ciuti, and J. Bloch, Probing a Dissipative Phase Transition via Dynamical Optical Hysteresis, *Phys. Rev. Lett.* **118**, 247402 (2017).
- [16] C. Lledó and M. Szymańska, A dissipative time crystal with or without Z_2 symmetry breaking, *New J. Phys.* **22**, 075002 (2020).
- [17] N. Carlon Zambon, S. R. K. Rodriguez, A. Lemaître, A. Harouri, L. Le Gratiet, I. Sagnes, P. St-Jean, S. Ravets, A. Amo, and J. Bloch, Parametric instability in coupled nonlinear microcavities, *Phys. Rev. A* **102**, 023526 (2020).
- [18] G. E. Astrakharchik and L. P. Pitaevskii, Motion of a heavy impurity through a Bose-Einstein condensate, *Phys. Rev. A* **70**, 013608 (2004).
- [19] A. Y. Cherny, J.-S. Caux, and J. Brand, Theory of superfluidity and drag force in the one-dimensional Bose gas, *Front. Phys.* **7**, 54 (2012).
- [20] A. Lichtenberg and M. Leiberman, *Regular and Stochastic Motion* (Springer, Berlin, 2013), Vol. 38.
- [21] R. Z. Sagdeev, D. A. Usikov, and G. M. Zaslavsky, *Nonlinear Physics: From the Pendulum to Turbulence and Chaos* (Harwood Academic Publishers, Reading, UK, 1988).
- [22] A. Giraldo, S. Masson, N. Broderick, and B. Krauskopf, Semi-classical bifurcations and quantum trajectories: A case study of the open Bose-Hubbard dimer, *Eur. Phys. J.: Spec. Top.* **231**, 385 (2022).
- [23] L. D. Landau and E. M. Lifshitz, *Mechanics*, Course of Theoretical Physics Vol. 1, 3rd ed. (Pergamon, New York, 1976), p. 93.
- [24] M. Shriali, A. Prasad, R. Ramaswamy, and U. Feudel, The nature of attractor basins in multistable systems, *Int. J. Bifurcation Chaos* **18**, 1675 (2008).
- [25] P. S. Muraev, D. N. Maksimov, and A. R. Kolovsky, Quantum manifestation of the classical bifurcation in the driven dissipative Bose-Hubbard dimer, [arXiv:2209.07029](https://arxiv.org/abs/2209.07029).
- [26] K. Vogel and H. Risken, Quasiprobability distributions in dispersive optical bistability, *Phys. Rev. A* **39**, 4675 (1989).
- [27] I. Carusotto and C. Ciuti, Quantum fluids of light, *Rev. Mod. Phys.* **85**, 299 (2013).
- [28] G. Kordas, S. Wimberger, and D. Witthaut, Decay and fragmentation in an open Bose-Hubbard chain, *Phys. Rev. A* **87**, 043618 (2013).
- [29] R. A. Kidd, M. K. Olsen, and J. F. Corney, Quantum chaos in a Bose-Hubbard dimer with modulated tunneling, *Phys. Rev. A* **100**, 013625 (2019).
- [30] S. Strogatz, From Kuramoto to Crawford: exploring the onset of synchronization in populations of coupled oscillators, *Physica D* **143**, 1 (2000).